

# Faraday Discussions

Accepted Manuscript



This manuscript will be presented and discussed at a forthcoming Faraday Discussion meeting. All delegates can contribute to the discussion which will be included in the final volume.

**Register now to attend!** Full details of all upcoming meetings: <http://rsc.li/fd-upcoming-meetings>



This is an *Accepted Manuscript*, which has been through the Royal Society of Chemistry peer review process and has been accepted for publication.

*Accepted Manuscripts* are published online shortly after acceptance, before technical editing, formatting and proof reading. Using this free service, authors can make their results available to the community, in citable form, before we publish the edited article. We will replace this *Accepted Manuscript* with the edited and formatted *Advance Article* as soon as it is available.

You can find more information about *Accepted Manuscripts* in the [Information for Authors](#).

Please note that technical editing may introduce minor changes to the text and/or graphics, which may alter content. The journal's standard [Terms & Conditions](#) and the [Ethical guidelines](#) still apply. In no event shall the Royal Society of Chemistry be held responsible for any errors or omissions in this *Accepted Manuscript* or any consequences arising from the use of any information it contains.

## ARTICLE

# A Computational Study of Potential Molecular Switches that Exploit Baird's Rule on Excited State Aromaticity and Antiaromaticity

Cite this: DOI: 10.1039/x0xx00000x

Received 00th January 2012,  
Accepted 00th January 2012

DOI: 10.1039/x0xx00000x

[www.rsc.org/](http://www.rsc.org/)H. Löfås,<sup>a</sup> B. O. Jahn,<sup>b</sup> J. Wärnå,<sup>a</sup> R. Emanuelsson,<sup>b</sup> R. Ahuja,<sup>a,c</sup> A. Grigoriev,<sup>a</sup>  
and H. Ottosson<sup>b</sup>

A series of tentative single-molecule conductance switches which could be triggered by light were examined by computational means using density functional theory (DFT) with non-equilibrium Green's functions (NEGF). The switches exploit the reversal in electron counting rules for aromaticity and antiaromaticity upon excitation from the electronic ground state ( $S_0$ ) to the lowest  $\pi\pi^*$  excited singlet and triplet states ( $S_1$  or  $T_1$ ), as described by Hückel's and Baird's rules, respectively. Four different switches and one antifuse were designed which rely on various photoreactions that either lead from the OFF to the ON states (switches **1**, **2** and **4**, and antifuse **5**) or from the ON to the OFF state (switch **3**). The highest and lowest ideal calculated switching ratios are 1175 and 5, respectively, observed for switches **1** and **4**. Increased thermal stability of the **1-ON** isomer is achieved by benzannulation (switch **1B-OFF/ON**). The effects of constrained electrode-electrode distances on activation energies for thermal hydrogen back-transfer from **1-ON** to **1-OFF** and the relative energies of **1-ON** and **1-OFF** at constrained geometries were also studied. The switching ratio is strongly distance dependent as revealed for **1B-ON/OFF** where it equals 711 and 148 when the ON and OFF isomers are calculated in electrode gaps with distances confined to either that of the OFF isomer or to that of the ON isomer, respectively.

## 1 Introduction

Molecules composed of a few dozens of atoms constitute the smallest objects that can be designed in an essentially unlimited number of versions and which also are stable at ambient conditions. For example, it has been estimated that  $10^{40}$  different molecules with sizes of a regular drug molecule can be designed based on the most common elements.<sup>1</sup> Thus, the combination of molecular chemistry and electronics provides for an exceptional wealth of design possibilities for the smallest possible memory and logic devices that are of such high stabilities that they potentially can be used in everyday applications.<sup>2,3</sup> The molecular switch is therefore a component that has received significant attention in the last decades, and a variety of different molecular switches have been reported,<sup>3-5</sup> activated with different kinds of external stimuli, such as light, force, heat, or as recently shown, the current running through a junction.<sup>6</sup> Light is a particularly attractive stimuli due to its fast response time and compatibility with already existing experimental setups.<sup>4</sup> The existing molecular switches can roughly be divided into two categories: isomerization switches,<sup>7-19</sup> where the three-dimensional structure (connectivity, configuration, or conformation) of the molecular

system is changed, or redox/polarization-switches,<sup>20-22</sup> where the molecule (or part of it) takes up or loses an electron. Our tentative molecular switches, studied through quantum chemical calculations reported herein, fall into the first category and they could presumably be stimulated by light in one direction and by heat in the other.

A major drawback for some of the previously studied molecular switches, *e.g.*, azobenzenes, is the fact that they change length during switching, making them unsuitable in solid state devices.<sup>8,7,11</sup> Furthermore, isomerization switches should ideally have the ON state represented by a planar compound with a linearly conjugated path with maximal  $p_\pi$ -orbital overlap. The compound representing the OFF state, on the other hand, should have a disruption in its  $\pi$ -conjugation, and such a disruption could be accomplished by a saturated molecular segment (*structural isomerization*) or by a large twist in the conjugated path (*stereoisomerization*), in the optimal case not changing the length. Furthermore, it should be possible to switch the molecule between the two states with external stimuli.

We argue that quantum chemical calculations should be efficient tools in the development of completely new classes of

molecular switch compounds. In the switch-design we exploit Baird's rule as a qualitative guiding tool.<sup>23-25</sup> This rule tells that the numbers of  $\pi$ -electrons needed for aromaticity and antiaromaticity, respectively, in the lowest  $\pi\pi^*$  excited singlet and triplet states ( $S_1$  and  $T_1$ ) of cyclic fully conjugated hydrocarbons (annulenes) are opposite to that of the electronic ground state ( $S_0$ ), described by Hückel's rule.<sup>26-29</sup> *I.e.*, annulenes with  $4n$   $\pi$ -electrons are aromatic and those with  $4n+2$   $\pi$ -electrons are antiaromatic in the  $T_1$  and  $S_1$  states. This rule was derived by Colin Baird in 1972 through use of perturbation molecular orbital (PMO) theory.<sup>23</sup> Since then it has been verified through a series of quantum chemical calculations using different aromaticity indices, and it has been shown to be valid also in the  $S_1$  state.<sup>30,31</sup> Yet, it is very seldom applied in the design of optically and photochemically active compounds.<sup>24,25</sup>

Following Baird's rule, compounds which are aromatic in  $S_0$  (*e.g.*, benzene) become antiaromatic upon excitation. Thus, they change character from being exceptionally stable to become more reactive, and for this reason we recently described benzene as a molecular "Dr. Jekyll and Mr. Hyde".<sup>25</sup> Indeed, the alleviation of the antiaromatic character of a benzene ring in its  $S_1$  and  $T_1$  states should be a driver for various photorearrangements in benzene derivatives, and this could be exploited for the identification of new compounds that may be applicable in single-molecule photoswitches. At this point it should be noted that our switch candidates either have essentially the same lengths in the ON and the OFF isomers, or they are conformationally highly flexible whereby only small energy penalties are needed for adjustment to electrode gaps that are not ideal for a specific isomer.

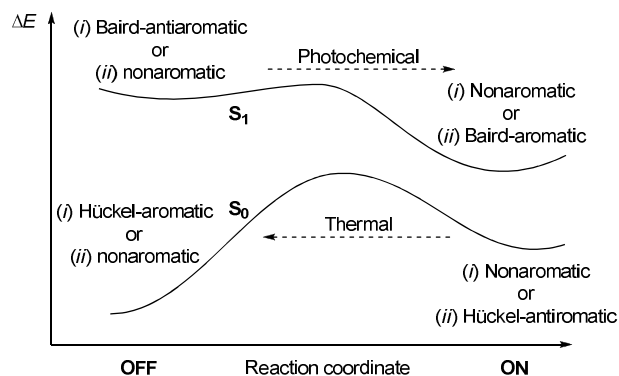
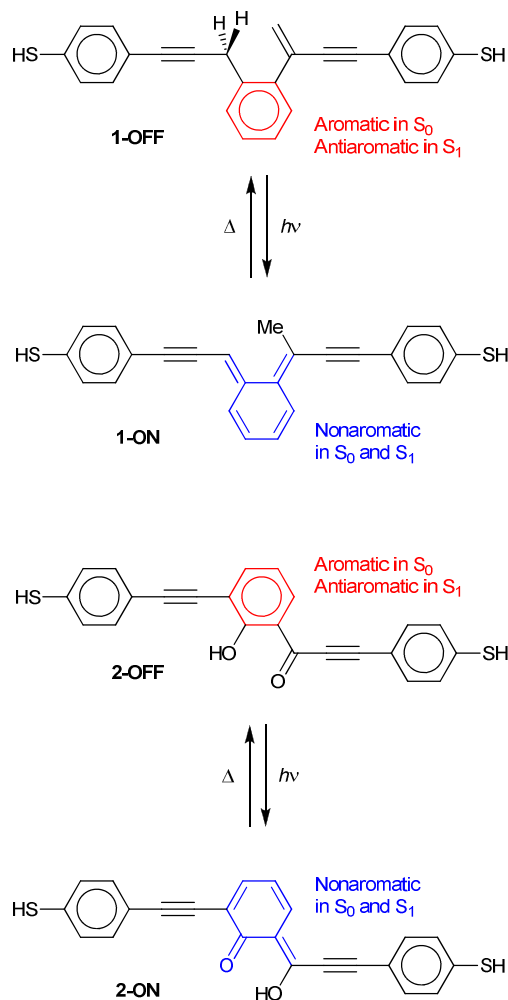


**Figure 1** The general shapes of the  $S_0$  and  $S_1$  potential energy surfaces and the expected influence of aromaticity, antiaromaticity and non-aromaticity at the various minima in the  $S_0$  and  $S_1$  states.

Two situations which are useful for molecular switches can be identified and that imply either decreased degree of antiaromaticity or increased degree of aromaticity along the reaction coordinates in both  $S_1$  and  $S_0$  (Figure 1). First are compounds which are  $S_0$  aromatic and  $S_1$  antiaromatic (Baird-antiaromatic), and that as a result of the latter are prone to

photorearrange to a non-aromatic isomer. The second class of compounds are nonaromatic in both their  $S_0$  and  $S_1$  states but can photorearrange so as to attain aromaticity in  $S_1$  (Baird-aromaticity). After decay to  $S_0$  these species may rearrange back to the start upon regain in  $S_0$  aromaticity and/or reduction in  $S_0$  antiaromaticity.

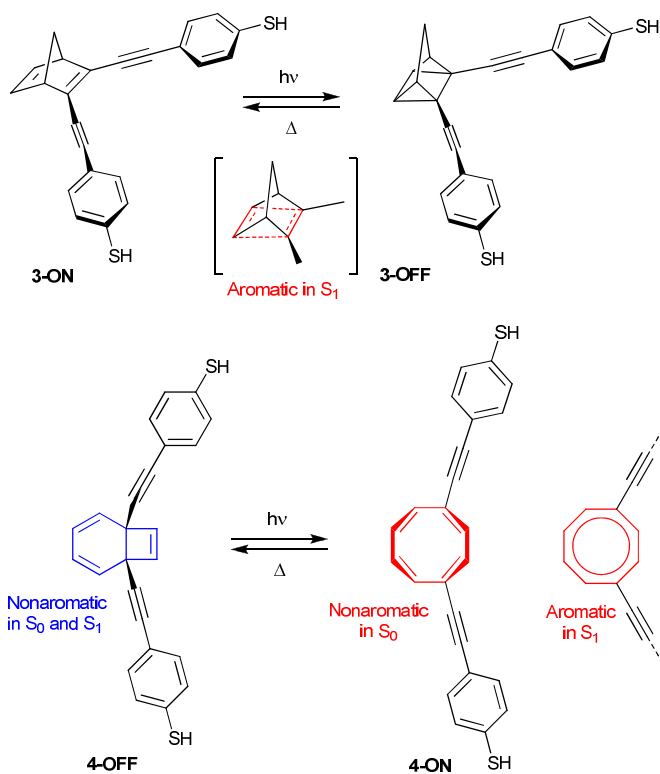


**Scheme 1** Potential molecular conductance switches based on photochemical hydrogen shifts in which the  $S_1$  state antiaromaticity is diminished through the photoreaction. The benzene ring which is the core of the photorearrangement of the OFF-state is shown in red, and the *ortho*-xylylene fragments found in the ON-states are shown in blue.

Photorearrangements of benzene derivatives could be useful in the design of new optical conductance switches provided the switches can be tailored so that the rearrangements lead from low-conducting to more highly conducting isomers. Photoinduced hydrogen shifts could be attractive in this context because with properly designed switching compounds the reaction may lead to only small length differences between the ON- and the OFF-isomers (states), as earlier concluded by Benesch *et al.*<sup>9</sup> Additionally, if the hydrogen back-transfer is hampered by the immobilization between the electrodes to the extent that back-transfer to the starting isomer (state) does not

occur spontaneously at ambient temperatures then the isomer pair could represent a new molecular switch type.

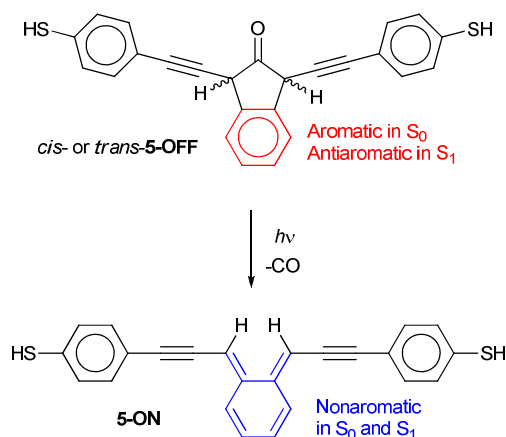
We have now investigated the transport properties of new types of tentative light-triggered molecular switches, where systems **1** and **2** are based on photochemical hydrogen-shifts (Scheme 1)<sup>32-35</sup> and systems **3** and **4** exploit two different pericyclic photoreactions (Scheme 2).<sup>36-39</sup> We also propose an "antifuse", **5**, based on a double Norrish Type I reaction leading to a photodecarbonylation (Scheme 3).<sup>40</sup> This optically activated "antifuse" is the opposite of a fuse as its electrically conductive path is opened when triggered by light of the appropriate wavelength. The general feature of switches **1**, **2** and the antifuse **5** is that the photoreactions induced by an  $S_1$  antiaromatic benzene ring lead to molecular fragments of *ortho*-xylylene type, providing for linearly  $\pi$ -conjugated paths through the molecules, and eliminated aromaticity in the  $S_0$  state. This should lead to a particularly high conductivity, in line with recent findings on the conductivities of compounds in which the degree of aromaticity of the central unit could be varied.<sup>41</sup> In the tentative switches **3** and **4** it is the gain in excited state  $4n\pi$ -electron aromaticity that drives the reactions forward.



**Scheme 2** Potential molecular conductance switches based on photochemical cycloaddition and electrocyclic ring-opening reactions in which the  $S_1$  state aromaticity is gained, in the case of **3** leading to a photocycloaddition.

At this point it should be noted that the presently reported switch candidates primarily represent templates for further

design. Still, it should be remarked that all of these tentative switches are based on molecules and reactions that have been studied experimentally in other contexts.<sup>32-40</sup> The photoreactions upon which the switch function in the specific candidates rely represent only a few of the reactions that likely can be used. Thus, the present investigation represents a start on the design of optical switches which exploit the opposite rules for aromaticity and antiaromaticity in the ground state *vs.* the lowest  $\pi\pi^*$  excited states.



**Scheme 3** A potential molecular antifuse based on Norrish Type I reaction in which  $S_1$  state antiaromaticity of the benzene ring marked red is diminished through photodecarbonylation leading to formation of an *ortho*-xylylene fragment marked in blue.

## 2 Computational Methods

The isolated molecules were first optimized by use of the B3LYP hybrid density functional theory with the 6-31G(d) valence double-zeta basis set.<sup>42-44</sup> These calculations were performed with the Gaussian09 program package.<sup>45</sup> The activation barriers for the thermal back-reactions were optimized without geometry constraints as well as at constrained S---S distances corresponding to those of either the ON or the OFF isomer.

The modelled device consists of three parts: left electrode, molecule, and right electrode. First, the relaxed molecular structures shown in Schemes 1 - 3 were inserted between two Au(111)-surfaces and relaxed with three gold layers on each side. To remove interactions between periodic images in the lateral dimensions, a  $6 \times 6$  supercell ( $17.5 \text{ \AA} \times 17.5 \text{ \AA}$ ) was used. For transport calculations three more layers of gold are added on each side at experimental bulk positions. All relaxations are performed at the DFT-level with the SIESTA package<sup>46,47</sup> and core electrons are modeled using Troullier-Martins<sup>48</sup> soft norm-conserving pseudo-potentials. The valence electrons are expanded in a basis set of local orbitals using a double-zeta plus

polarization orbitals (DZP) basis set for electrons in the molecule and a single-zeta plus polarization orbitals (SZP) basis set for electrons in the gold electrode. The GGA of Perdew-Burke-Ernzerhof was used for the exchange-correlation functional.<sup>49</sup> Transport calculations were carried out from first principles with a method based on non-equilibrium Green's functions (NEGF) combined with DFT as implemented in the TranSIESTA package.<sup>50</sup> The zero-bias transmission,  $T = T(E)$ , was calculated at the Fermi energy  $E_F$  and sampled over a  $12 \times 12$  k<sub>||</sub>-mesh.

### 3 Results and Discussion

To analyze the switching behaviour in the reactions outlined in Schemes 1 - 3, we first calculated the electronic transport of the ON and OFF isomer pairs of the various switch candidates, attached to gold electrodes, in the framework of DFT-NEGF. In these first calculations the most extended conformations of the molecules were chosen. The zero-bias transmissions for the different compounds are shown in Figures 2, 4, 6, 8 and 9 where each panel shows the transmission for the ON and the OFF isomers (states) for the different switch candidates. The results for the zero-bias conductance together with switching ratios (SR) at  $V = 0$  and the length in the junction of the most extended conformation of the compounds (S---S distances) are collected in Table 1.

Subsequently, we analyze how realistic the switches are. In particular we examined (i) if the activation energies for thermal back-reactions are sufficiently high to allow the ON (or OFF) isomer to be persistent at ambient temperatures, and (ii) what effect constrained electrode-electrode distances have on the transport properties and SRs of the systems found to have the highest idealized SRs. We also explored further derivatisations of the switches which could lead to higher thermal stability of the ON as well as the OFF isomers.

**Table 1:** Conductance characteristics of switches

Compound	Conductance <sup>a</sup> ( $G_0$ )	SR <sup>b</sup>	S---S distance <sup>c</sup>
<b>1-ON</b>	$3.4 \times 10^{-4}$		20.6
<b>1-OFF</b>	$2.9 \times 10^{-4}$	1175	20.7
<b>2-ON</b>	$6.6 \times 10^{-2}$		20.9
<b>2-OFF</b>	$1.2 \times 10^{-4}$	548	20.8
<b>3-ON</b>	$2.8 \times 10^{-1}$		12.0
<b>3-OFF</b>	$6.1 \times 10^{-3}$	47	11.7
<b>4-ON</b>	$5.9 \times 10^{-3}$		11.4
<b>4-OFF</b>	$1.1 \times 10^{-3}$	5	12.2
<b>5-ON</b>	$2.8 \times 10^{-1}$		20.40
<i>cis</i> - <b>5-OFF</b>	$4.5 \times 10^{-4}$	623	19.42
<i>trans</i> - <b>5-OFF</b>	$6.3 \times 10^{-4}$	450	19.42

<sup>a</sup> Conductance at zero bias (0 V).

<sup>b</sup> Conductance ON/OFF switching ratio at zero bias (0 V).

<sup>c</sup> Distance between thiol end-groups [Å].

#### 3.1 Switches based on photoinduced hydrogen-transfer

Switch **1** is based on a photochemically induced antarafacial [1,5]-sigmatropic H-shift, and this reaction converts **1-OFF**,

having one saturated  $sp^3$  C atom and a cross-conjugated segment, into **1-ON** having a linearly conjugated path spanning the complete molecule. For this switch there are large differences between the two isomers. For **1-OFF** the HOMO-level is positioned far from  $E_F$  and there is a large antiresonance in the transmission function about 0.9 eV below  $E_F$ . On the other hand, with the extended conjugation in **1-ON** the HOMO shifts closer to  $E_F$  and, at the same time, the HOMO-LUMO gap is decreased to give high transmission over the whole energy range considered in Figure 2.

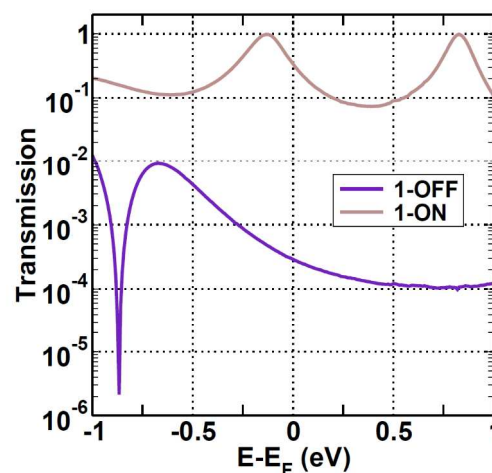


**Figure 2:** Transmission spectra ( $V = 0$ ) for switch **1** shown in Scheme 1.

The differences for the HOMO and LUMO levels in the ON and OFF states are clearly seen in the plot of the spatial distribution of the density of states in the junction (see Figure 3). For **1-OFF** the HOMO-level is about 0.5 eV below  $E_F$  and mostly localized to the two conjugated phenylethynyl segments with a very weak connection through the central part of the molecule. In contrast, the HOMO of **1-ON** is shifted close to  $E_F$  and it is delocalized over the complete molecule. Also, the LUMO level is now visible  $\sim 1$  eV above  $E_F$ . Thus, for **1** there is both a shift of the most conducting level closer to  $E_F$  as well as a delocalization of the level over the complete molecule when going from the OFF to the ON-state. This has been shown earlier to give a high switching ratio,<sup>15</sup> and this is also the case here as an idealized switching ratio of nearly twelve-hundred was calculated (Table 1). Noteworthy, the large anti-resonance in **1-OFF** can be traced back to destructive interference introduced by cooperative effects of the cross-conjugated unit and the central  $S_0$ -state aromatic benzene ring, seen as reversal of the local currents in this segment at the energy of the antiresonance (see the Supplementary Information).

The second switch based on an intramolecular hydrogen-shift is **2**. The **2-OFF** isomer has a low conductance (Figure 4) which should be due to (i) the cross-conjugated connectivity around the carbonyl group, and (ii) the *meta*-substitution pattern around the  $S_0$  aromatic benzene ring. Similar as for switch **1**, the benzene ring promotes a H-shift lowering the  $S_1$



antiaromaticity. This leads to a central (non-aromatic) *ortho*-xylylene derivative **2-ON** which has a linearly conjugated path between the two electrodes. The compounds have previously been studied experimentally, however, the corresponding ON-state is a short-lived transient species.<sup>35</sup> Thus, the usage of these or similar compounds in molecular switch applications need further tailoring.

where the local currents in **1-ON** and **2-ON** are shown. For **1-ON** there are two well-conducting linearly conjugated paths through the central *ortho*-xylylene unit, one short butadiene path and one long octatetraene path. In contrast, the shorter path in **2-ON** is disrupted by the cross-conjugated carbonyl segment and the current follows the longer conjugated path. Despite this, **2** has a reasonably high switching ratio of approximately five-hundred (Table 1).

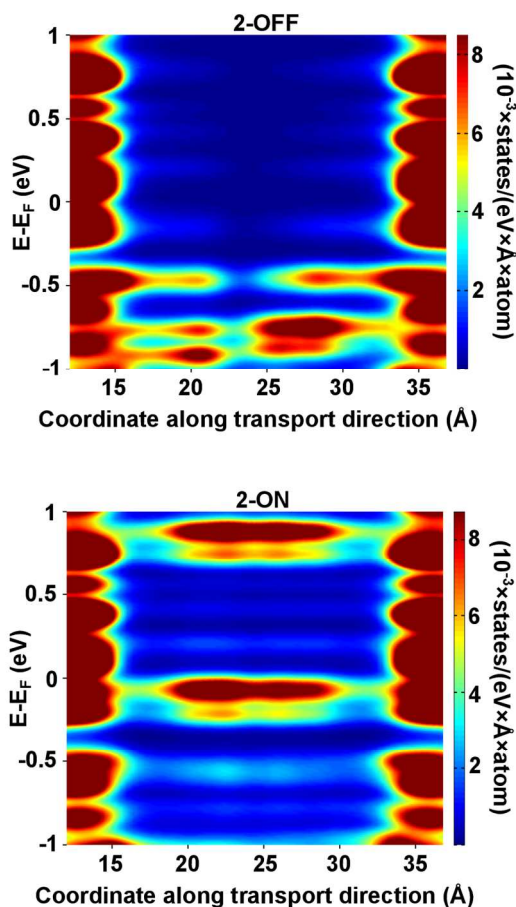


Figure 3 PDOS for **1-OFF** and **1-ON**.

The charge transport characteristic of **2** is very similar to that of **1**. The overall conductances of both **2-OFF** and **2-ON** are lower compared to the corresponding isomers of **1**, yet, it is known that *meta*-substituted benzene rings give lower transmissions.<sup>51,52</sup> Similar as for **1**, the aromatic ring in **2** which is *meta*-substituted together with the cross-conjugated segment around the carbonyl group lowers the transmission in **2-OFF** significantly compared to the fully conjugated **2-ON**.<sup>53,54</sup> The **2-OFF** also has a deep antiresonance about 1 eV above  $E_F$  introduced by interference in the *meta*-substituted benzene which leads to an even further decrease in the transmission at  $E_F$ . Moreover, the lower conductance of **2-ON** when compared to **1-ON** can be explained by the cross-conjugated carbonyl moiety which reduces the number of linearly conjugated paths through the *ortho*-xylylene unit. This can be seen in Figure 5

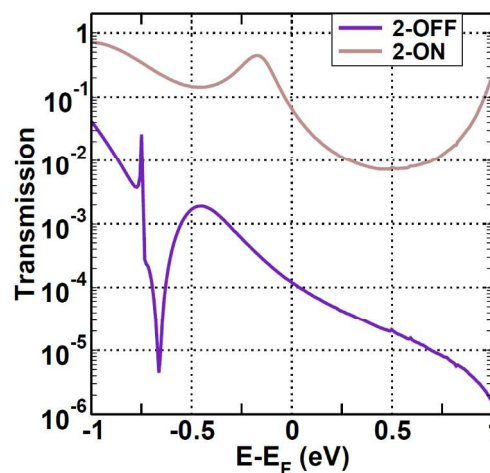


Figure 4: Transmission spectra ( $V = 0$ ) for switch **2** shown in Scheme 1

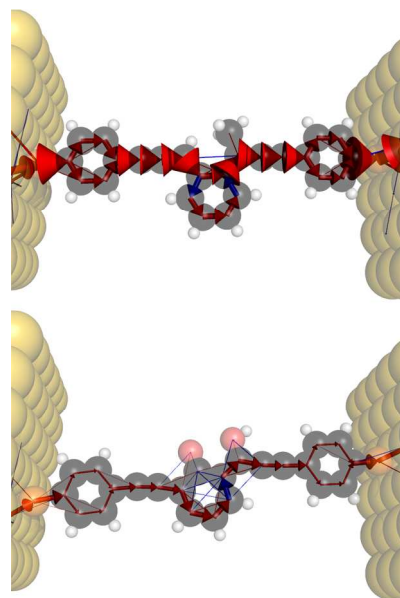


Figure 5: Local currents in **1-ON** (top) and **2-ON** (bottom), where the cross-sectional area of the cylinder is proportional to the current density. Red currents represent positive transport direction, and blue currents represent negative direction. The currents are calculated at the Fermi energy  $((\mu_L + \mu_R)/2)$ , but a small positive bias voltage is assumed for computational purposes. For a full derivation see Okabayashi et. al.<sup>55</sup> and Paulsson et. al.<sup>56</sup> In order to become visible, the local currents in **2** is magnified with a factor two compared to **1**.

### 3.2 Switches based on ring-closure/opening reactions

Two different photochemical reactions that lead to/from cyclic (partially) saturated molecular segments were also examined as bases for tentative switches; (i) the [2+2] photocycloaddition leading from a norbornadiene to a quadricyclane, and (ii) a photochemical electrocyclic ring-opening leading from a bicyclo[4.2.0]octa-2,4,7-triene to a cyclooctatetraene. Noteworthy, while the photoreactions of **1**, **2**, **4** and **5** lead from an OFF state to an ON state, the photoreaction of **3** leads from the ON to the OFF state.

We first consider **3** which is based on the norbornadiene to quadricyclane photoisomerization. In **3-ON** one of the C=C double bonds of the norbornadiene unit provides a conjugated path while the quadricyclane unit of the **3-OFF** is a fully saturated hydrocarbon which ideally should disrupt the  $\pi$ -conjugation. Noteworthy, the electron transfers through norbornadiene and quadricyclane moieties have been examined experimentally earlier through intervalence electron transfer studies using a *bis*(pentaamine-ruthenium(II)) complex of dicyanonorbornadiene.<sup>36,37</sup> The effective coupling through the dicyanonorbornadiene ligand was determined to 0.023 eV, however, no intervalence transition could be found for the corresponding quadricyclane complex.

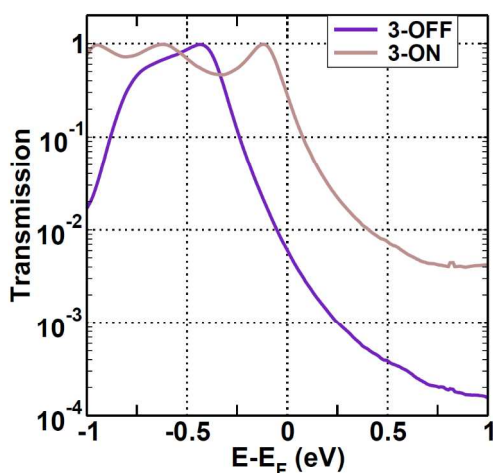


Figure 6: Transmission spectra ( $V = 0$ ) for the switch **3** shown in Scheme 2.

Here, the transmissions of **3-ON** and **3-OFF** show similar behaviours with broad peaks in the DOS from HOMOs close to  $E_F$ , which give high transmissions for both isomers (Figure 6). The thermal cycloreversion which leads from **3-OFF** to the **3-ON** shifts the HOMO level even closer to  $E_F$ , making it almost resonant. Nonetheless, due to the high transmission of the OFF-isomer this results in a moderate switching ratio of about fifty for the **3-ON/OFF** isomer pair. The high transmission of **3-OFF** is possibly due to the two strained cyclopropane rings in the quadricyclane fragment providing bent bond orbitals which can overlap with the  $\pi$ -orbitals of the phenylethynyl arms. Indeed, when viewing the HOMOs of the isolated **3-ON** and **3-**

**OFF** (Figure 7, top), respectively, one can note that the central norbornadiene/quadricyclane core contributes significantly in both cases and that the orbital energies differ by only 0.23 eV, in approximate agreement with the difference in the positions of the resonance transmission in Figure 6. The local currents at the Fermi level are also significant through the central quadricyclane moiety of **3-OFF** (Figure 7, bottom) and increases as the energy is off-set.

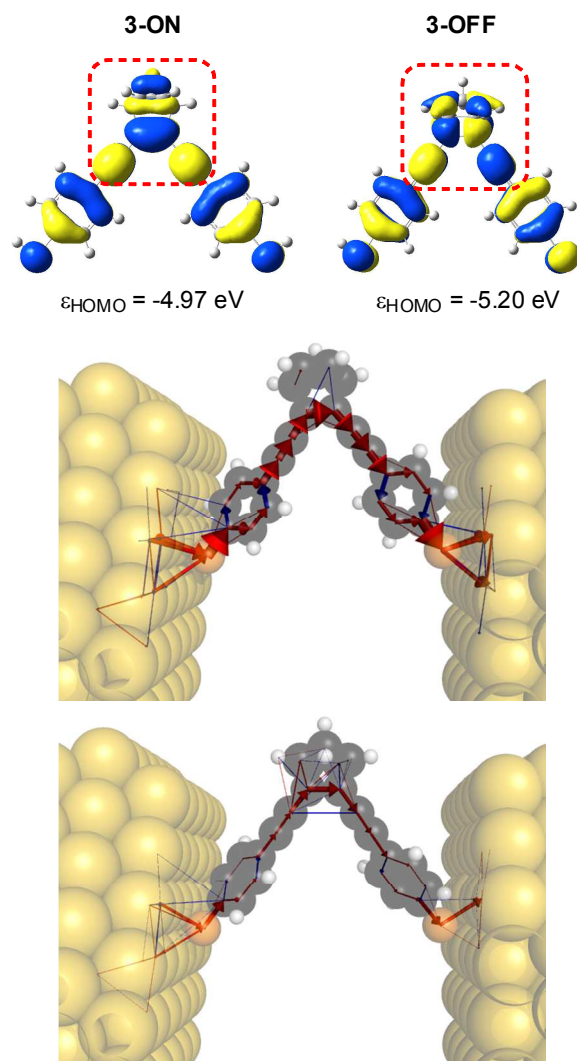


Figure 7: (top) Orbital plots of the HOMOs of **3-OFF** and **3-ON** at B3LYP/6-31G(d) level with the central norbornadiene (**3-ON**) or quadricyclane (**3-OFF**), and the two adjacent ethynyl segments, encircled in red. The symmetry notations of the HOMOs are *b* (**3-ON**) and *a* (**3-OFF**), respectively, in the  $C_2$  point group. (Middle and bottom frames) Local currents in **3-ON** (middle) and **3-ON** (bottom), where the cross-sectional area of the cylinder is proportional to the current density. Red currents represent positive transport direction, and blue currents represent negative direction. The currents are calculated at the Fermi energy  $((\mu_L + \mu_R)/2)$ , but a small positive bias voltage is assumed for computational purposes. For a full derivation see Okabayashi et. al.<sup>55</sup> and Paulsson et. al.<sup>56</sup> In order to become visible, the local currents in **3-OFF** is magnified by a factor 20 compared to **3-ON**.

The next switch, **4**, has a similar behavior to **3** with a broad DOS close to  $E_F$  from the HOMO level (Figure 8), with a slight shift between **4-ON** and **4-OFF**. The introduction of the two

cyclic units in the bicyclo[4.2.0]octatri-2,4,7-ene moiety creates destructive interference in **4-OFF** showing up as an antiresonance about 0.7 eV below  $E_F$ . Here the interference can be traced back to a reversal of the currents in the four-membered ring-segment including the central C-C single bond. The moderate conductance of **4-ON** gives a very low ON/OFF ratio of merely five, and it is likely due to the poor conjugative  $p_\pi$ -overlap because of a puckered tub-shaped structure of the cyclooctatetraene ring.

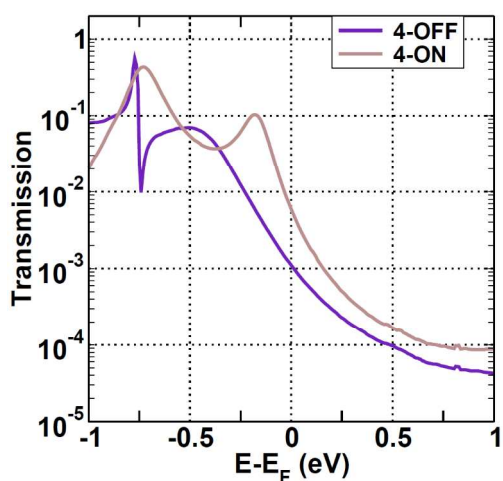


Figure 8: Transmission spectra ( $V = 0$ ) for the switch **4** shown in Scheme 2.

### 3.3 An antifuse based on photodecarbonylation

The last compound pair considered, **5** (Scheme 3), is not a molecular switch but an antifuse. The **5-OFF** and **5-ON** compounds are also not isomers, and the photoreaction is irreversible as carbon monoxide leaves. Here, the OFF-state is a molecule with the current path disrupted by two  $sp^3$  hybridized C atoms. The photoinitiated decarbonylation leading to the conducting **5-ON** state can be viewed as a result of (i) the double  $\alpha$ -cleavage (Norrish Type I) of the C-C bonds adjacent to the carbonyl group, as well as (ii) a way for the  $S_1$  state benzene ring to alleviate its destabilizing antiaromaticity. The  $S_1$ -antiaromatic character of the benzene ring presumably facilitates the decarbonylation. The linear conjugation introduced in **5-ON** increases the transmission (Figure 9), and the result is very close to **1-ON**, except that LUMO is shifted minutely closer to  $E_F$  as a result of the cross-conjugated  $C=CH_2$  instead of  $C=CHMe$  moiety.

Noteworthy, depending on whether one considers the *cis*- or the *trans*-isomer of **5-OFF**, the ON/OFF ratio is either about six-hundred or four-hundred fifty. The *cis*-**5-OFF** isomer is the least conducting according to our calculations. However, the *cis*-**5-OFF** isomer is not suitable because when formation of **5-ON** in a junction with electrode-electrode distance constrained to the *cis*-**5-OFF** is studied computationally it becomes clear that a **5-ON** isomer formed from *cis*-**5-OFF** would close

instantaneously to a low-conducting benzocyclobutene moiety with two saturated (insulating) C atoms.

### 3.4 Conclusions from transmissions at ideal situations

Among the five switch/antifuse candidates investigated only **1**, **2** and **5** have sufficiently high SR, and these compounds were analyzed further. None of these are, however, perfect as a molecular switch because the *ortho*-xylylene isomers (**1-ON**, **2-ON**, and **5-ON**) will most likely only be transient species. Immobilization between electrodes may decrease their potential to undergo dimerization reactions, however, may also facilitate the back-reactions to the corresponding OFF isomers. In addition, the experimental situation as such is complicated by a series of factors. The electrode-electrode distance is unclear, and the effects of stabilizing features in **1**, **2** and **5** on the conductance are also rather unclear.

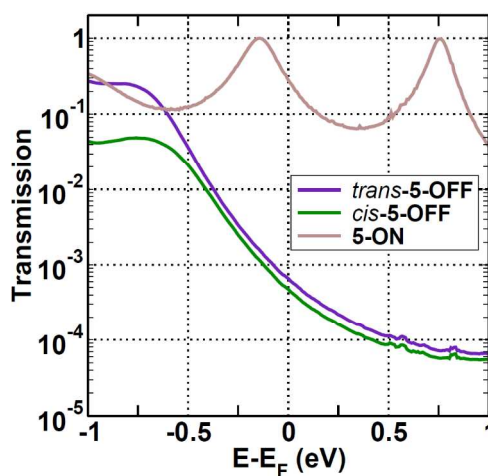


Figure 9: Transmission spectra ( $V = 0$ ) for the antifuse **5** shown in Scheme 3.

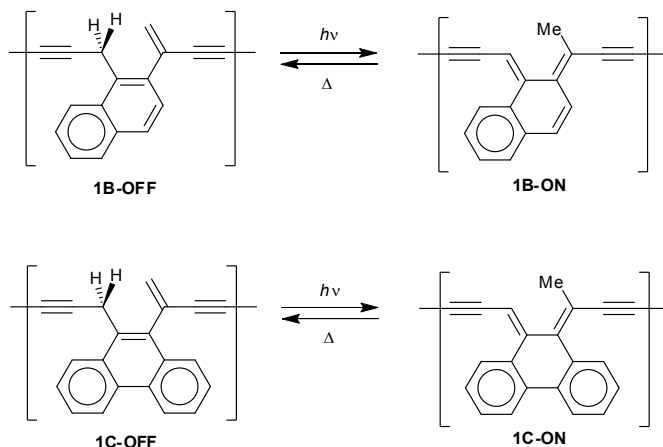
### 3.5 Thermal interconversion processes

The realization of the isomer pairs to operate as molecular switches relies on the existence of two stable isomers. As we want the switching process to progress by light in one direction and heat in the other there should also be energetic drive towards the starting isomer in the  $S_0$  state (OFF for **1**, **2** and **4**, and ON for **3**). Thus, we first examined the activation barriers for the thermal back-rearrangements from **1-ON** and **2-ON** to **1-OFF** and **2-OFF**, respectively. We also probed how to raise the activation barriers for these rearrangements above 120 kJ/mol, which should lead to a stable isomer at ambient temperatures. In addition to the parent switch-pairs **1-ON/OFF** and **2-ON/OFF** we therefore examined modified switch-pairs with either benzannulation to the central rearranging moiety (**1-ON/OFF**, Scheme 4) or with oxygen atoms exchanged to sulphur (**2-ON/OFF**). For a full list of the investigated switches see the Supplementary Information. One conclusion from these calculations is that the free energies of activation for the thermal hydrogen shift from **1-ON** to **1-OFF** can be modified



extensively; from 88.4 kJ/mol in **1-ON/OFF** to 104.5 and 126.4 kJ/mol in the switch pairs **1B-ON/OFF** and **1C-ON/OFF**, respectively, shown in Scheme 4. The corresponding transition state structure for the hydrogen shift from **1-OFF** to **1-ON** is displayed in Figure 10, top panel.

In contrast, the barriers for the hydrogen back-transfers in all derivatives of **2-ON/OFF** switches are too low (within the range 17.8 – 57.5 kJ/mol). Also, the transition state structures correspond to rotation about the C-O bond to the hydroxyl group rather than a shift of the H atom (Figure 10, bottom). The only substitution which has a substantial effect is the exchange of the hydroxyl group of **2-ON/OFF** to a methyl group and exchange of the carbonyl group to a vinyl group because this leads to an ON state with a significantly higher activation barrier for hydrogen back-transfer (~80 kJ/mol). However, this is still lower than our desired barrier height. Interestingly, and in contrast to the observation for **1B-ON/OFF** and **1C-ON/OFF**, further benzannulation lowered the barrier. For that reason focus in the next is placed exclusively on derivatives of **1-ON/OFF**.



**Scheme 4** The modified switches of type **1-ON/OFF** with benzannulation to increase the thermal stabilities of the OFF-isomers (states).

Furthermore, the restriction with fixed electrode-electrode distances will also influence the activation barriers for the hydrogen back-transfer reactions. Yet, rather than regarding the complete set of the various derivatives of switches we considered the change in the activation energy of switch **1-ON/OFF** at electrode-electrode distances which are optimal either for the ON isomer or for the OFF-isomer (Figure 10, middle structures). When the S---S distance is kept at the optimal OFF distance (17.191 Å) then  $\Delta G^\ddagger(298\text{ K}) = 116.2$  kJ/mol, while at the optimal ON-distance (20.303 Å)  $\Delta G^\ddagger(298\text{ K}) = 145.1$  kJ/mol. The lower activation energy for the shorter constrained S---S distance is in line with Hammond's postulate as this transition state structure is more OFF-like, and thus, lower in relative energy than the more ON-like transition state structure at more extended S---S distances. The energy needed

to adjust **1-OFF** to an S---S distance corresponding to that of the ON-isomer is merely 3.5 kJ/mol. Hence, the procedure in a tentative experiment should be to insert **1-OFF** into an electrode gap which is larger by ~3 Å than the length of **1-OFF** at its most stable conformer.

The energy of **1-ON** relative to that of **1-OFF** is 42.3 kJ/mol at the optimal S---S ON distance but just 5.5 kJ/mol at the optimal OFF distance. Again, it is apparent that it is ideal to keep the **1-ON/OFF** at the S---S distance of the ON isomer as this creates the largest energetic drive for return to the OFF isomer in the  $S_0$  state.

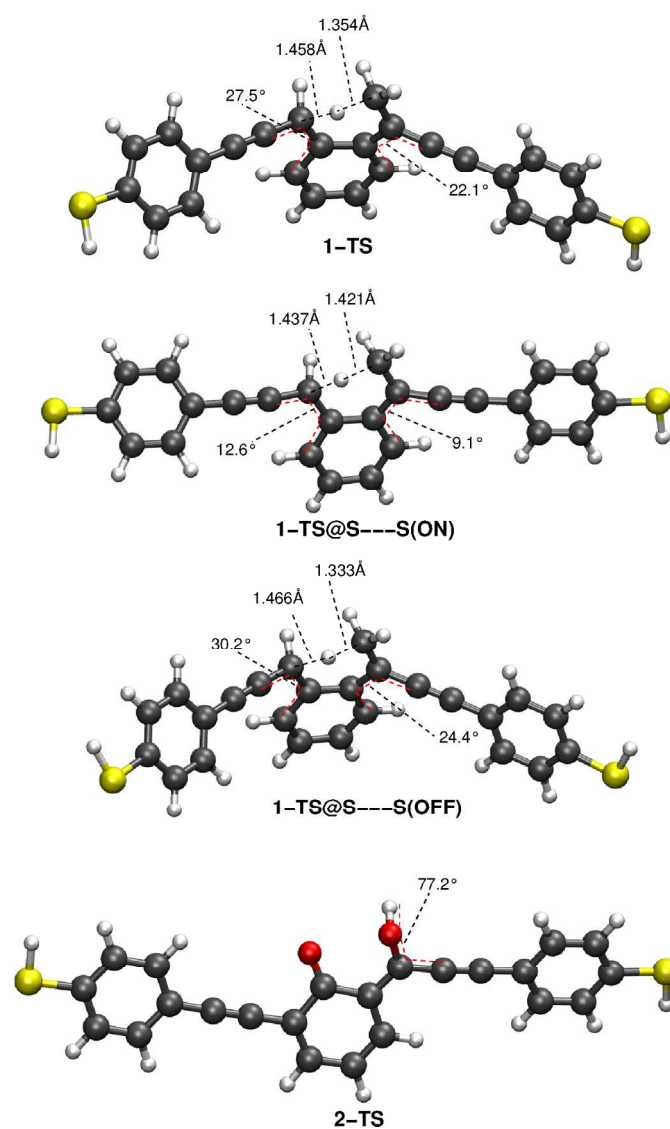


**Figure 10:** Transition state structures for thermal hydrogen back-transfer from **1-ON** to **1-OFF**, and from **2-ON** to **2-OFF**. Calculations at B3LYP/6-31G(d) level.

### 3.6 Effects on transport upon derivatization and electrode-electrode distance variation

Since both the **1-ON** and **1-OFF**, as well as the corresponding isomers of **1B** and **1C**, are conformationally flexible they should potentially be able to fit into electrode-electrode gaps which have slightly different gap distances than ideal for a certain isomer. Here we particularly examined switch **1B-ON/OFF** as this should have higher thermal stability of the ON isomer than the parent **1-ON/OFF** switch (activation energies for hydrogen back-transfer is 104.5 kJ/mol). For this switch the  $\Delta H(298\text{K})$  needed to compress **1B-ON** to the S---S distance of **1B-OFF** is 6.8 kJ/mol, and the  $\Delta H(298\text{K})$  to elongate **1B-OFF** to that of **1B-ON** is 11.4 kJ/mol. We also examined the transport properties of **1B-ON** and **1B-OFF** when confined to electrode gaps ideal for either the ON or the OFF isomer (Figure 11). From these computations it becomes clear that the transmission at zero-bias voltage of the OFF isomer is more geometry-dependent than the transmission of the ON isomer. The zero-bias transmissions of both the ON and OFF isomers are highest when the isomers are kept at lengths which are ideal for the opposite isomer, and these transmissions are higher by factors 1.4 and 3.4, respectively, than when the isomers are kept at their optimal lengths. A high switching ratio is clearly possible for **1B-ON/OFF** when kept at the OFF-distance (SR = 711) while that at the ON-distance is moderate (SR = 148). Here a comparison to other optically activated molecular conductance switches should be made. A class of switches which has been examined both experimentally and computationally is various diarylethene switches.<sup>10-15,18,19</sup> The experimentally determined single-molecule switching ratios for various derivatives are found in the range 6 – 300,<sup>13,15</sup> and the calculated ones vary from negligible to a few hundreds.<sup>18,19</sup> Thus, **1B-ON/OFF** displays a high ratio which should motivate future experimental investigations. Yet, the SR is still far below that of the recent dimethyl-hydropyrene/cyclophanediene (DHP/CPD) studied experimentally by Royal, Wandlowski and co-workers and which have SR > 10<sup>4</sup>.<sup>17</sup>

Indeed, it should be noted that the DHP/CPD switch can be turned photochemically in both directions, and both processes can be rationalized by an alleviation of excited state antiaromaticity.<sup>25</sup> In the OFF→ON state by alleviation of 14 $\pi$ -electron S<sub>1</sub> antiaromaticity and in the ON→OFF state by alleviation of the 6 $\pi$ -electron S<sub>1</sub> antiaromaticity of the two benzene rings.

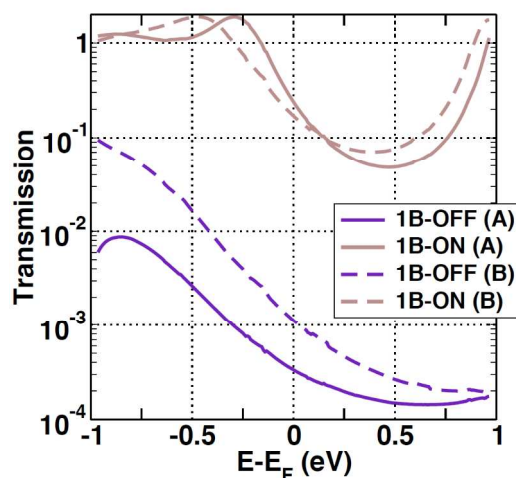


Figure 11: Transmissions through **1B-OFF** and **1B-ON** at electrode-electrode distances which are optimal for (A) **1B-OFF** and (B) **1B-ON**.

## Conclusions and Outlook

Aromaticity and antiaromaticity effects in the lowest  $\pi\pi^*$  excited singlet or triplet states (S<sub>1</sub> and T<sub>1</sub>) of fully conjugated carbocycles, as given by Baird's rule (aromaticity (antiaromaticity):  $4n$  ( $4n+2$ )  $\pi$ -electrons), can be applied for the design of new classes of photochemically triggered molecular conductance switches. The tendency of an excited state antiaromatic benzene ring to rearrange its substituent pattern so as to break the cyclic  $\pi$ -conjugation into an acyclic linearly  $\pi$ -conjugated *ortho*-xylylene, or a heteroderivative, is exploited in the first two switches, **1** and **2**, as well as in the antifuse **5**. These systems display calculated ideal ON/OFF switching ratios in the range 550 - 1175. This is, however, the maximal switching ratio, and lower ratios are to be expected as the molecules when in a junction presumably will adopt conformations with reduced  $p_\pi$ -overlap and thus weaker  $\pi$ -conjugation in the ON isomer (state). For this reason we analyzed the transmission of a benzannulated derivative of switch **1** (**1B-ON/OFF**), and found that particularly the transmission of the OFF isomer was strongly dependent on geometry.

We also investigated two tentative molecular switches where we exploit the favourable involvement of excited state aromatic  $4n\pi$ -electron cycles. Such cycles are formed during the photochemical [2+2] cycloaddition of norbornadiene to quadricyclane, leading from **3-ON** to **3-OFF**, and in photochemical retrocyclizations of bicyclo[4.2.0]octa-2,4,7-triene to cyclooctatetrane, leading from **4-OFF** to **4-ON**. In both of these switches the OFF state has two saturated sp<sup>3</sup> carbon atoms which are converted to sp<sup>2</sup> hybridized C atoms, however, it should be noted that the photorearrangements lead from the ON to the OFF state in the first switch and from the OFF to the ON state in the second one. Still, neither **3** nor **4** possess high ON/OFF ratios.

To conclude, molecular switches of type **1-ON/OFF** should be particularly interesting for experiments. Such experimental studies should resolve both the photophysical and photochemical properties of the molecular switches, the thermal stabilities, and the charge transport characteristics.

Although this present investigation is exclusively computational, some general guidelines can be drawn based on our findings. Besides the fact that rearrangements leading from isomers that contain cross-conjugated and/or saturated molecular segments to isomers with linearly conjugated paths are desirable a few additional generalizations can also be made. Saturated cyclopropyl units bridging two  $\pi$ -conjugated segments may only be saturated in a formal sense as the local Walsh orbitals of the cyclopropyl groups can interact with the  $\pi$ -orbitals of the unsaturated segments. Moreover, large annulene moieties, e.g., a cyclooctatetraene unit, which pucker should be avoided in the ON state for the apparent reason that the  $\pi$ -conjugation through such units is weakened. Finally, it could be desirable if the OFF isomer is conformationally flexible, as in **1-OFF**, so that it can adjust to an electrode-electrode gap with some variation in the gap distance with only a small energy penalty.

### Acknowledgements

We gratefully acknowledge Uppsala University through funding of the U3MEC KoF07-initiative, the Swedish Research Council (Vetenskapsrådet), Carl Tryggers Stiftelse för Vetenskaplig Forskning, the Wenner-Gren Foundations, the Swedish Energy Agency, and Stiftelsen för Strategisk Forskning (SSF (SUSBATT)) for financial support. The calculations were performed on resources provided by the Swedish National Infrastructure for Computing (SNIC) at C3SE and NSC.

### Notes and references

<sup>a</sup> Department of Physics and Astronomy, Uppsala University, Box 516, SE-75120, Uppsala, Sweden.

<sup>b</sup> Department of Chemistry - BMC, Uppsala University, Box 576, SE-75123, Uppsala, Sweden.

<sup>c</sup> Applied Materials Physics, Department of Materials and Engineering, Royal Institute of Technology (KTH), SE-10044, Stockholm, Sweden.

Electronic Supplementary Information (ESI) available: Interference of **1-OFF**, full reference 41, energy tables and Cartesian coordinates. See DOI: 10.1039/b000000x/

- P. Ball, *Nature*, 2006, **442**, 500–502.
- H. Song, M. A. Reed, and T. Lee, *Adv. Mater.*, 2011, **23**, 1583–1608.
- S. J. van der Molen and P. Liljeroth, *J. Phys.: Condens. Matter*, 2010, **22**, 133001.
- N. Fuentes, A. Martín-Lasanta, L. Álvarez de Cienfuegos, M. Ribagorda, A. Parra, and J. M. Cuerva, *Nanoscale*, 2011, **3**, 4003.
- M. Galperin and A. Nitzan, *Phys. Chem. Chem. Phys.*, 2012, **14**, 9421–9438.
- C. Schirm, M. Matt, F. Pauly, J. C. Cuevas, P. Nielaba, and E. Scheer, *Nat. Nanotechnol.*, 2013, **8**, 645–648.
- M. Alemani, M. V. Peters, S. Hecht, K.-H. Rieder, F. Moresco, and L. Grill, *J. Am. Chem. Soc.*, 2006, **128**, 14446–14447.
- B.-Y. Choi, S.-J. Kahng, S. Kim, H. Kim, H. Kim, Y. Song, J. Ihm, and Y. Kuk, *Phys. Rev. Lett.*, 2006, **96**, 156106.
- C. Benesch, M. F. Rode, M. Čížek, R. Härtle, O. Rubio-Pons, M. Thoss, and A. L. Sobolewski, *J. Phys. Chem. C*, 2009, **113**, 10315–10318.
- S. J. van der Molen, J. Liao, T. Kudernac, J. S. Agustsson, L. Bernard, M. Calame, B. J. van Wees, B. L. Feringa, and C. Schönenberger, *Nano Lett.*, 2009, **9**, 76–80.
- K. Smaali, S. Lenfant, S. Karpe, M. Oçafraïn, P. Blanchard, D. Deresmes, S. Godey, A. Rochefort, J. Roncali, and D. Vuillaume, *ACS Nano*, 2010, **4**, 2411–2421.
- S. Lara-Avila, A. V. Danilov, S. E. Kubatkin, S. L. Broman, C. R. Parker, and M. B. Nielsen, *J. Phys. Chem. C*, 2011, **115**, 18372–18377.
- Y. Kim, T. J. Hellmuth, D. Sysoiev, F. Pauly, T. Pietsch, J. Wolf, A. Erbe, T. Huhn, U. Groth, U. E. Steiner, and E. Scheer, *Nano Lett.*, 2012, **12**, 3736–3742.
- Y. Kim, A. Garcia-Lekue, D. Sysoiev, T. Frederiksen, U. Groth, and E. Scheer, *Phys. Rev. Lett.*, 2012, **109**, 226801.
- Jia, C., Wang, J., Yao, C., Cao, Y., Zhong, Y., Liu, Z., Liu, Z., Guo, X. *Angew. Chem. Int. Ed.* 2013, **52**, 8666–8670.
- H. Löfås, A. Orthaber, B. O. Jahn, A. M. Rouf, A. Grigoriev, S. Ott, R. Ahuja, and H. Ottosson, *J. Phys. Chem. C*, 2013, **117**, 10909–10918.
- Roldan, D.; Kaliginedi, V., Cobo, S., Kolisoska, V., Bucher, C., Hong, W., Royal, G., Wandlowski, T. *J. Am. Chem. Soc.* 2013, **135**, 5974–5977.
- Odell, A., Delin, A., Johansson, B., Rungger, I., Sanvito, S. *ACS Nano*, 2010, **4**, 2635–2642.
- Tsujii, Y., Hoffmann, R. *Angew. Chem.* 2014, **126**, 4177–4181.
- F. Chen, J. He, C. Nuckolls, T. Roberts, J. E. Klare, and S. Lindsay, *Nano Lett.*, 2005, **5**, 503–506.
- L. Bogani and W. Wernsdorfer, *Nat. Mat.*, 2008, **7**, 179–186.
- J. Liao, J. S. Agustsson, S. Wu, C. Schönenberger, M. Calame, Y. Leroux, M. Mayor, O. Jeannin, Y.-F. Ran, S.-X. Liu, and S. Decurtins, *Nano Lett.*, 2010, **10**, 759–764.
- N. C. Baird, *J. Am. Chem. Soc.*, 1972, **94**, 4941–4948.
- H. Ottosson, *Nat. Chem.*, 2012, **4**, 969–971.
- M. Rosenberg, C. Dahlstrand, K. Kilså, and H. Ottosson, *Chem. Rev.*, 2014, **114**, 5379–5425.
- E. Hückel, *Grundzüge der Theorie Ungesättigter und Aromatischer Verbindungen*, Verlag Chemie GmbH, Berlin, 1938.
- V. I. Minkin, M. N. Glukhovtsev, and B. Y. Simkin, *Aromaticity and antiaromaticity: Electronic and Structural Aspects*, John Wiley and Sons Ltd, New York, 1994.
- P. v. R. Schleyer, *Chem. Rev.*, 2001, **101**, 1115–1118.
- N. Martin, M. M. Haley, and R. R. Tykwinski, *Chem. Commun.*, 2012, **48**, 10471–10471.
- P. B. Karadakov, *J. Phys. Chem. A*, 2008, **112**, 12707–12713.
- P. B. Karadakov, *J. Phys. Chem. A*, 2008, **112**, 7303–7309.
- M. Moreno, R. Gelabert, J. M. Lluch, and J. M. Ortiz Sánchez, *Phys. Chem. Chem. Phys.*, 2013, **15**, 20236–20246.
- A. C. Pratt, *J. Chem. Soc., Chem. Commun.*, 1974, 183–184.
- S. V. Kessar, T. Singh, and A. K. S. Mankotia, *J. Chem. Soc., Chem. Commun.*, 1989, 1692.
- S. J. Formosinho and L. G. Arnaut, *J. Photochem. Photobiol. A: Chem.*, 1993, **75**, 21–48.
- P. Lainé, V. Marvaud, A. Gourdon, J.-P. Launay, R. Argazzi, and C.-A. Bignozzi, *Inorg. Chem.*, 1996, **35**, 711–714.
- S. Fraysse, C. Coudret, and J.-P. Launay, *Eur. J. Inorg. Chem.*, 2000, **2000**, 1581–1590.
- D. Bryce-Smith and J. E. Lodge, *Proc. Chem. Soc.*, 1961, 333.
- J. E. Garbe and V. Boekelheide, *J. Am. Chem. Soc.*, 1983, **105**, 7384–7388.
- K. K. De Fonseca and J. J. McCullough, *J. Am. Chem. Soc.*, 1979, **101**, 3277–3282.
- W. Chen, H. Li, J. R. Widawsky, C. Appayee, L. Venkataraman, and R. Breslow, *J. Am. Chem. Soc.* 2014, **136**, 918.
- A. D. Becke, *J. Chem. Phys.* 1993, **98**, 1372–1377.
- P. J. Stephens, F. J. Devlin, C. F. Chabalowski, M. J. Frisch, *J. Phys. Chem.* 1994, **98**, 11623–11627.
- P. C. Hariharan, J. A. Pople *Theor. Chim. Acta* 1973, **28**, 213–222.
- Gaussian 09, Revision C.01 and D.01, M. J. Frisch *et al.*, Gaussian

- Inc. Wallington CT, 2009. For the complete reference see Electronic Supplementary Information.
46. J. M. Soler, E. Artacho, J. D. Gale, A. Garcia, J. Junquera, P. Ordejon, and D. Sánchez-Portal, *J. Phys.: Condens. Matter*, 2002, **14**, 2745–2779.
  47. E. Artacho, E. Anglada, O. Diéguez, J. D. Gale, A. García, J. Junquera, R. M. Martín, P. Ordejon, J. M. Pruneda, D. Sanchez-Portal, and J. M. Soler, *J. Phys.: Condens. Matter*, 2008, **20**, 064208.
  48. N. Troullier and J. L. Martins, *Phys. Rev. B*, 1991, **43**, 1993–2006.
  49. J. P. Perdew, K. Burke, and M. Ernzerhof, *Phys. Rev. Lett.*, 1996, **77**, 3865–3868.
  50. M. Brandbyge, J.-L. Mozos, P. Ordejon, J. Taylor, and K. Stokbro, *Phys. Rev. B*, 2002, **65**, 165401.
  51. M. Mayor, H. B. Weber, J. Reichert, M. Elbing, C. von Hänisch, D. Beckmann, and M. Fischer, *Angew. Chem., Int. Ed.*, 2003, **42**, 5834–5838.
  52. T. Hansen, G. C. Solomon, D. Q. Andrews, and M. A. Ratner, *J. Chem. Phys.*, 2009, **131**, 194704.
  53. M. Ernzerhof, H. Bahmann, F. Goyer, M. Zhuang, and P. Rocheleau, *J. Chem. Theory Comput.*, 2006, **2**, 1291–1297.
  54. G. C. Solomon, C. Herrmann, T. Hansen, V. Mujica, and M. A. Ratner, *Nat. Chem*, 2010, **2**, 223–228.
  55. N. Okabayashi, M. Paulsson, H. Ueba, Y. Konda, and T. Komeda, *Phys. Rev. Lett.*, 2010, **104**, 077801.
  56. M. Paulsson and M. Brandbyge, *Phys. Rev. B*, 2007, **76**, 115117.